Atmospheric
Chemistry
and Physics

Supplement of

Investigation of several proxies to estimate sulfuric acid concentration under volcanic plume conditions

Clémence Rose et al.

*Correspondence to:* Clémence Rose (c.rose@opgc.univ-bpclermont.fr)

1. Temperature-dependant reaction rate constant between SO_2 and OH

The temperature-dependant reaction rate k (cm^3 molecule^{-1} s^{-1}) between SO_2 and OH is given by DeMore et al. (1997) and Sander et al. (2002):

$$k = \frac{A \times k_3}{(A + k_3)} \times \exp\left\{ k_5 \times \left[1 + \log_{10}\left(\frac{A}{k_3}\right)^2 \right]^{-1} \right\} \tag{S1}$$

where $A = k_1 \times [M] \times \left(\frac{300}{T}\right)^{k_2}$, $[M] = 0.101 \times (1.381 \times 10^{-23} \times T)^{-1}$ is the density of air (molecule cm^{-3}), $k_1 = 4 \times 10^{-31}$, $k_2 = 3.3$, $k_3 = 2 \times 10^{-12}$ and $k_5 = -0.8$.

2. Correlations between $[H_2SO_4]$ and key atmospheric variables
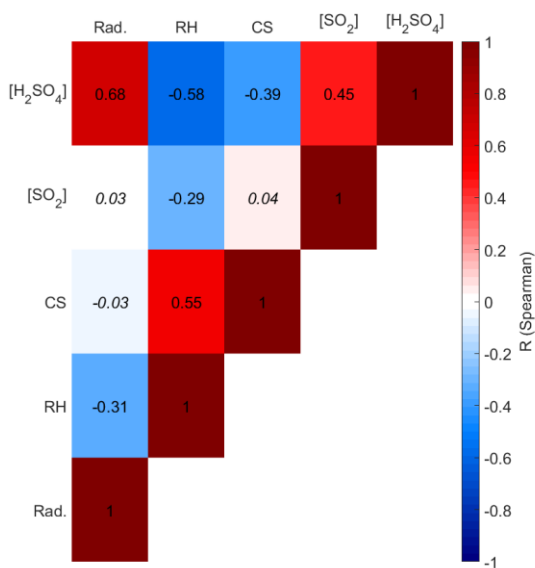
Fig. S1 Correlation coefficients (Spearman) between $[H_2SO_4]$ and the key atmospheric variables likely affecting H_2SO_4 formation in the eruptive volcanic plume of the Piton de la Fournaise during OCTAVE. The correlation coefficients are indicated by the colour code for a quick overview, and corresponding values are in addition reported on the figure for each couple of variables. Values highlighted in italic indicate non-statistically significant correlations (i.e. corresponding p-value was > 0.05).
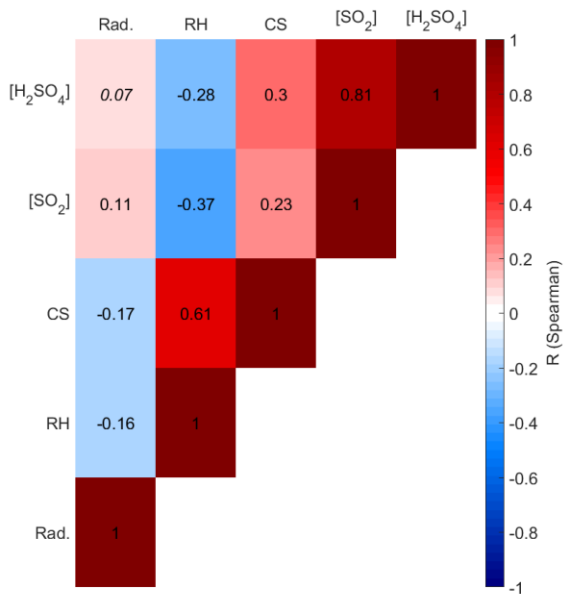
Fig. S2 Correlation coefficients (Spearman) between [H_2SO_4] and the key atmospheric variables likely affecting H_2SO_4 formation in the passive degassing plume of Etna during the first part of flight ETNA 13 in STRAP. See Fig. S1 for an explanation of the symbols.

3. Derivation of the proxies using measurements performed in the volcanic eruption plume of the Piton de la Fournaise during OCTAVE – Effect of including [O_3] in the proxies

Table S1 Fit results after replacing global radiation by the product Rad $\times$ [O_3] in all the proxies. Note that the procedure was only applied to the original dataset (no bootstrap resampling). For simplicity, the results are reported separately for the three proxy families: a) F1-F3, which are the proxies with powers fixed to -1 or 1 for all variables, b) A1-A4, which have individual adjusted powers for each variable and c) S1, which includes the additional H_2SO_4 sink related to cluster formation. Note that based on corresponding p-values, all correlations were found significant ($p < 0.05$).
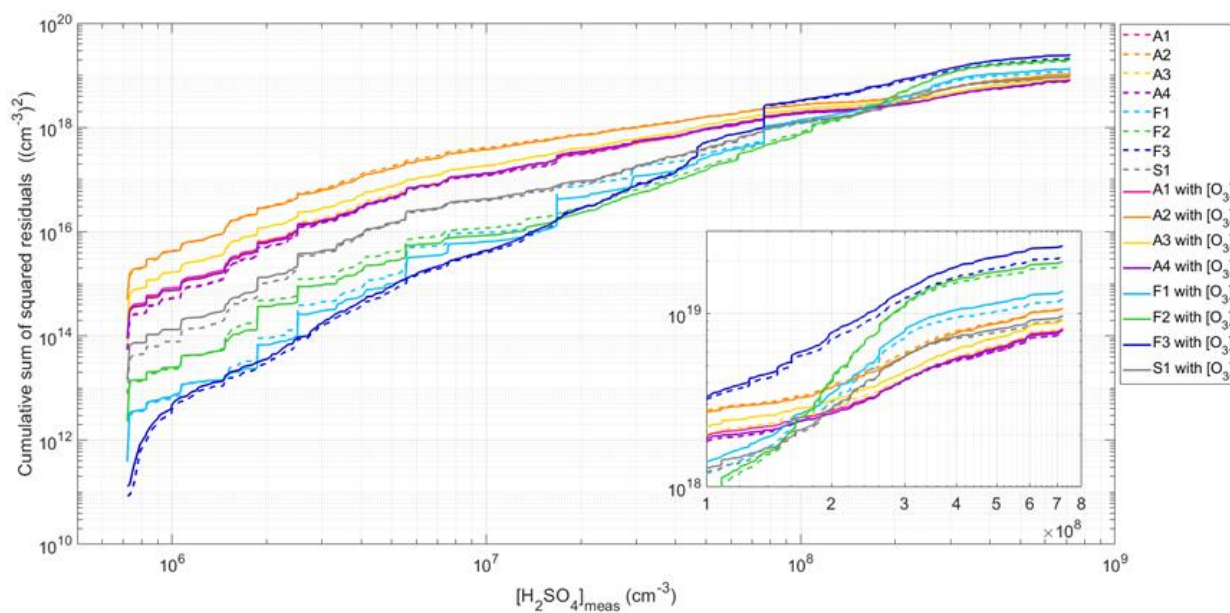
a)

4. Proxy	K	R	RE	SSR ($\times 10^{19}$ (molec. cm^{-3})^2)
F1	1.49×10^{-9}	0.68	0.52	1.35
F2	2.81×10^{-7}	0.54	0.64	1.99
F3	3.51×10^{-8}	0.43	0.75	2.45

b)

Proxy	a	b	c	d	e	f	R	RE	SSR ($\times 10^{19}$ (molec. cm^{-3})^2)
A1	1.44×10^{-10}	0.77	0.47	-0.47	-	-	0.78	0.45	0.82
A2	3.19×10^{-6}	0.61	0.39	-	-		0.70	0.56	1.07
A3	1.13×10^{-7}	0.68	0.42	-	-0.22		0.75	0.49	0.92
A4	1.36×10^{-11}	0.80	0.49	-0.53	-	0.15	0.79	0.44	0.80

c)

Proxy	α	β	R	RE	SSR ($\times 10^{19}$ (molec. cm^{-3})^2)
S1	4.91×10^{-9}	2.78×10^{-11}	0.74	0.46	0.97

5

Fig. S3 Cumulative sum of squared residuals associated to the different proxies, with (solid lines) and without (dashed lines) the inclusion of [O$_3$] in the corresponding functions. The insert presents a zoom into the results obtained for [H2SO4] $> 1\times10^8$ cm^{-3}.
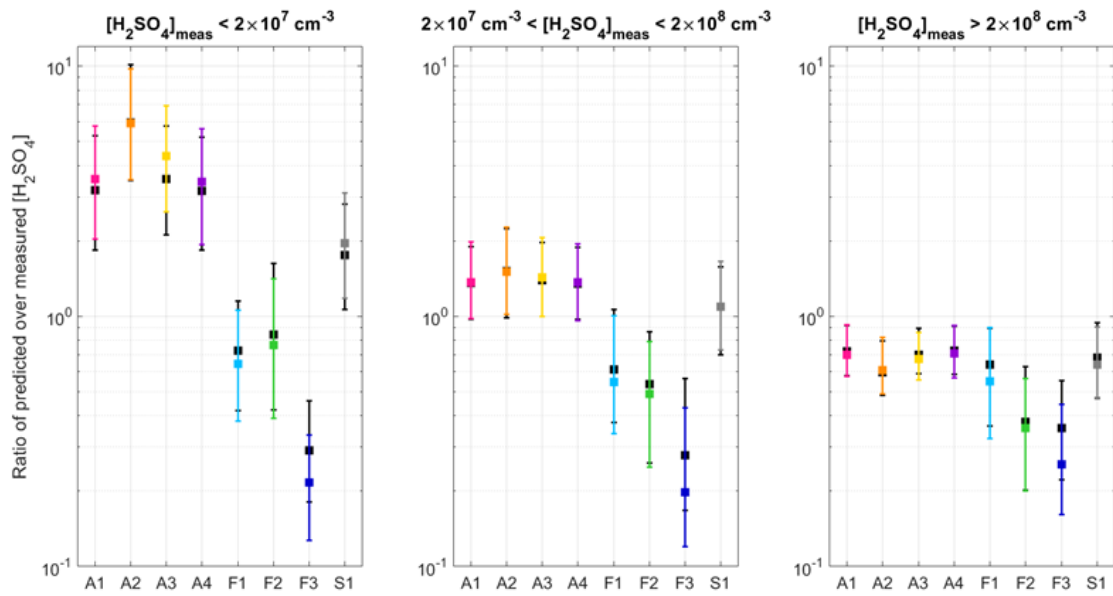
10

Fig. S4 Ratio between predicted and measured $[H_2SO_4]$ in the different $[H_2SO_4]$ subranges. For each proxy, the coloured marker represents the median of the ratio obtained when accounting for $[O_3]$ in the prediction, and lower and upper limit of the corresponding error bar indicate the 25th and 75th percentiles, respectively. Black markers and error bars correspond to the results shown in Fig. 5, *i.e.* in absence of $[O_3]$ in the proxies.